Original Article

Berberine mitigates hepatic insulin resistance by enhancing mitochondrial architecture via the SIRT1/Opa1 signalling pathway

Jia Xu[1,†], Yining Zhang[3,†], Zhiyi Yu[1], Yueqi Guan[1], Yuqian Lv[1], Meishuang Zhang[1], Ming Zhang[1], Li Chen[1], Xiaoyan Iv[2,*], and Fengying Guan[1,*]

[1]Department of Pharmacology, School of Basic Medical Sciences, Jilin University, Changchun 130021, China, [2]Department of Clinical Laboratory, the Second Clinical Hospital Affiliated to Jilin University, Changchun 130041, China, and [3]Department of Pediatric Endocrinology, the First Clinical Hospital Affiliated to Jilin University, Changchun 130021, China

[†]These authors contributed equally to this work.

*Correspondence address. Tel: +86-431-85619799; E-mail: guanfy@jlu.edu.cn (F.G.) / Tel: +86-431-81136607; E-mail: williams1980@jlu.edu.cn (X.L.)

Abstract

The aberrant changes of fussion/fission-related proteins can trigger mitochondrial dynamics imbalance, which cause mitochondrial dysfunctions and result insulin resistance (IR). However, the relationship between the inner mitochondrial membrane fusion protein optic atrophy 1 (Opa1) and hepatic IR as well as the specific molecular mechanisms of signal transduction has not been fully elucidated. In this study, we explore whether abnormalities in the Opa1 cause hepatic IR and whether berberine (BBR) can prevent hepatic IR through the SIRT1/Opa1 signalling pathway. High-fat diet (HFD)-fed mice and db/db mice are used as animal models to study hepatic IR *in vivo*. IR, morphological changes, and mitochondrial injury of the liver are examined to explore the effects of BBR. SIRT1/Opa1 protein expression is determined to confirm whether the signalling pathway is damaged in the model animals and is involved in BBR treatment-mediated mitigation of hepatic IR. A palmitate (PA)-induced hepatocyte IR model is established in HepG2 cells *in vitro*. Opa1 silencing and SIRT1 overexpression are induced to verify whether Opa1 deficiency causes hepatocyte IR and whether SIRT1 improves this dysfunction. BBR treatment and SIRT1 silencing are employed to confirm that BBR can prevent hepatic IR by activating the SIRT1/Opa1 signalling pathway. Western blot analysis and JC-1 fluorescent staining results show that Opa1 deficiency causes an imbalance in mitochondrial fusion/fission and impairs insulin signalling in HepG2 cells. SIRT1 and BBR overexpression ameliorates PA-induced IR, increases Opa1, and improves mitochondrial function. SIRT1 silencing partly reverses the effects of BBR on HepG2 cells. SIRT1 and Opa1 expressions are downregulated in the animal models. BBR attenuates hepatic IR and enhances SIRT1/Opa1 signalling in db/db mice. In summary, Opa1 silencing-mediated mitochondrial fusion/fission imbalance could lead to hepatocyte IR. BBR may improve hepatic IR by regulating the SIRT1/Opa1 signalling pathway, and thus, it may be used to treat type-2 diabetes.

Key words berberine, hepatic insulin resistance, SIRT1, Opa1, mitochondrial architecture

Introduction

Mitochondria provide ATP to cells [1] and play a key role in cellular energy metabolism. Mitochondrial dysfunction results in various metabolic diseases, including IR and type 2 diabetes [2], and is characterised by damaged substrate oxidation and impaired mitochondria accumulation, which are related to an imbalance in mitochondrial fusion/fission [1,3]. A few GTPase family proteins are involved in mammalian mitochondrial fusion/fission.

Outer mitochondrial membrane (OMM) fusion proteins include mitofusin (Mfn) 1 and 2, whereas Opa1 is an inner mitochondrial membrane (IMM) fusion protein. Dynamin-related protein 1 (Drp1) and fission protein 1 (Fis1) are involved in mitochondrial fission [4].

The roles of Mfn1, Mfn2, and Drp1 in hepatic IR have been investigated. Sameer et al. [5] reported that Mfn1 deficiency in the liver protects against diet-induced IR. David et al. [6] observed that liver-specific Mfn2 KO mice had impaired glucose tolerance, enhanced hepatic gluconeogenesis, and impaired insulin sensitivity. Wang et al. [7] observed that liver-specific Drp1 KO mice showed decreased fat mass and resistance to high-fat diet (HFD)-induced obesity. However, the relationship between Opa1 and hepatic IR as well as the specific molecular mechanisms of signal transduction has not been fully elucidated.

Opa1 is a dynamin-related GTPase that plays a dual role in mediating IMM fusion and maintaining the crista structure [8]. The human Opa1 protein is encoded by a single gene consisting of 30 exons. Alternative splicing at the N-terminal exons 4, 4b, and 5b generates 8 mRNA variants [9]. Opa1 precursors are expressed as several spliced variants, and their translocation to the mitochondria is associated with proteolytic processing of the amino-terminal presequence to the IM-anchored form L-Opa1. The transmembrane domain of L-Opa1 is further cleaved to form peripheral S-Opa1, which leads to mitochondrial fragmentation [10]. In the steady state, L-Opa1 coexists with S-Opa1. In damaged mitochondria, the majority of L-Opa1 is converted to S-Opa1, and the fusion activity is lost [11]. Ban et al. [10] found that the presence of L-Opa1 on one side of the membrane and that of cardiolipin on the other side are sufficient for fusion.

Sirtuin 1 (silent information regulator-1, SIRT1) regulates multiple biological processes such as glucose-lipid metabolism and mitochondrial biogenesis [12]. SIRT1 can modulate hepatic glucose metabolism by interacting with PGC-1α and directly increasing insulin sensitivity in the liver under different pathological conditions [13]. Jung et al reported [14] that an increase in SIRT1 expression could ameliorate PA-induced hepatocyte IR. SIRT1 plays a key role in mitochondrial biogenesis through PGC-1α acetylation/deacetylation [15]. Recent studies have revealed that SIRT1 regulates the transcription of Drp1 through PGC-1α in diabetic hearts [16]. However, the role of SIRT1 in Opa1 regulation is unknown.

BBR is the main active ingredient of Coptis root, which has multiple pharmacologic effects, including anti-inflammatory, anti-hypertensive and antioxidation effects [17,18]. Moreover, it can accelerate glucose transport, increase glycogen synthesis, regulate glucose metabolism, and improve hepatic IR [19]. Many studies have explored whether BBR can improve mitochondrial function. Qin et al. [20] revealed that BBR could protect glomerular podocytes by inhibiting Drp1-mediated mitochondrial fission and dysfunction. Ana et al. [21] provided evidence that BBR stimulates mitochondrial biogenesis through a SIRT1-mediated mechanism.

In the present study, we investigated the relationship between Opa1 and hepatic IR in the absence of Opa1 activation and examined whether SIRT1 regulates Opa1 to improve PA-induced hepatocyte IR with SIRT1 activation and Opa1 silencing in HepG2 cells. Finally, we explored whether BBR can improve hepatic IR by activating the SIRT1/Opa1 pathway through SIRT1 silencing.

Materials and Methods
Animal care
Three-week-old male C57BL/6J mice (HFK Bioscience, Beijing, China) weighing 14–16 g were raised in a standard temperature- and humidity-controlled environment with a 12:12-h light:dark cycle for a week before experiments. The mice had access to nesting material and were provided ad libitum access to water and a commercial low-fat diet (LFD, 10% fat; Research Diets, New Brunswick, USA) or high-fat diet (HFD, 60% fat; Research Diets) for 10 weeks.

Seven-week-old male db/db mice (average weight: 41 g) and C57BL/6J mice (average weight: 22 g) were purchased from the Model Animal Research Centre of Nanjing University (Nanjing, China) and adaptively raised for a week in an environment similar to that for the C57BL/6J mice. These db/db mice were fed with a regular diet for 4 weeks. In the control (CON) group, the C57BL/6J mice were given normal saline (10 mL/kg body weight). The db/db mice were randomly divided into two groups. In the model group (db/db) and BBR group, the diabetic mice were administered with normal saline (10 mL/kg body weight) and BBR (160 mg/kg body weight), respectively. The intragastric mode of administration was used in our study. The BBR dosage used in our experiment was chosen according to previous animal studies and clinical trials [22]. Mice body weight and fasting blood glucose (FBG) were measured weekly. Low-density lipoprotein cholesterol (LDL), triglycerides (TG), total cholesterol (T-CHO), fasting blood insulin, glucose-stimulated insulin secretion (GSIS), oral glucose tolerance test (OGTT) and insulin tolerance test (ITT) were performed at the end of the experiment.

Determination of OGTT, ITT, and GSIS
The C57BL/6J mice were fed with LFD and HFD for 10 weeks, and the db/db mice were fed with a regular diet for 4 weeks. All mice were starved for 12 h before the OGTT. Approximately 10 μL of blood was drawn from the mouse tail tip, and the OGTT was performed using test strips (Roche, Basel, Switzerland) and a glucometer (Roche). After orally administering 40% glucose (2 g/kg body weight; Xilong Scientific Company, Foshan, China) to the mice, their blood glucose was tested at 0, 30, 60, 90, and 120 min. For the ITT, the db/db mice were starved for 2 h and then administered with insulin (0.5 IU/kg body weight, i.p.; Novolin R; Novo Nordisk A/S, Copenhagen, Denmark). Blood glucose was measured at 0, 15, 30, 60, and 120 min. For the GSIS test, blood was drawn from the iliac vein of the C57BL/6J mice at 0 and 30 min, and the insulin level was measured using the Mouse Ultrasensitive Insulin ELISA kit (80-INSMSU-E01; ALPCO, Salem, USA) according to the manufacturer's instructions.

Haematoxylin-Eosin staining
The mice were anesthetized with 1.5% isoflurane. Subsequently, their liver tissue was removed at 4°C, washed with ice-cold PBS solution, and then fixed in 10% formaldehyde solution for one day. The tissue was dehydrated with a conventional gradient alcohol series and embedded in paraffin. The sections were 5 μm thick. After dewaxing and hydration, haematoxylin dyeing, dehydration, and neutral gum sealing, a good field of view was selected to observe and capture photographs using a BX53 fluorescence microscope (Olympus, Tokyo, Japan).

Electron microscopy
Liver samples obtained from the db/db mice were minced and placed in a fixative solution comprising 2.5% glutaraldehyde and 2% paraformaldehyde in 0.1 M cacodylate buffer (pH 7.4) for 2 h at 4°C. These samples were postfixed in 1% osmium tetraoxide buffer for 1.5 h. The liver samples were then dehydrated using alcohol, embedded in Epon, and cut into sections of 80-nm thickness. The liver sections were then photographed using an X-650 electron

microscope (Hitachi, Tokyo, Japan), and the mitochondria in the hepatic cells were observed for morphology analysis.

Cell culture and transfection

HepG2 cells (Genetic Testing Biotechnology, Suzhou, China) were cultured in DMEM containing 4.5 g/L glucose (Gibco, Grand Island, USA) supplemented with 10% FBS (Clark, Richmond, USA). After 24 hours passaging and reaching about 70% confluence, cells were transfected with transfection reagent lipofectamine 2000 (Invitrogen, Shanghai, China) according to manufacturer's instructions. Firstly, si-RNA, plasmid, Mito-DsRed (Addgene, Watertown, USA) and lipofectamine 2000 were added to serum-free Opti-MEM medium (Gibco) and mixed for 5 min. Then the diluted si-RNA, plasmid and Mito-DsRed were added to the diluted lipofectamine 2000 (1:1 ratio). After 15 min incubation at room temperature, the mixture was added to the corresponding wells of the culture plate containing an appropriate amount of Opti-MEM medium. After 4-6 h of transfection, DMEM containing 4.5 g/L glucose (containing 10% FBS) was used to change the medium. The Opa1 siRNA sequence (5′-GATCATCTGCCACGGGTTGTT-3′), SIRT1 siRNA sequence (5′-ACUUUGCUGUAACCCUGUAUU-3′) and overexpression plasmid were purchased from GenePharma (Shanghai, China). Negative control (5′-UUCUCCGAACGUGUCACGUTT-3′) for siRNA was also provided by GenePharma.

Immunofluorescence assay

HepG2 cells were grown on glass coverslips and mitochondrial morphology was visualized by overexpressing the mitochondrially targeted Mito-DsRed protein. One day after Mito-DsRed transfection, the culture medium was discarded and washed with PBS. The cells were fixed with 4% paraformaldehyde and incubated on ice for 10 min. The coverslips were mounted with nail polish and viewed with a confocal laser scanning microscope (Carl Zeiss, Oberkochen, Germany).

Cell viability assay

HepG2 cells were adjusted to a density of 5×10^3 cells/mL and cultured in a 96-well microplate. After treatment with different concentrations of PA and BBR for 24 h, 20 µL of the 5 mg/mL MTT solution (Sigma, St Louis, USA) was added to each well, and the cells were incubated for 3 h. Then, 200 µL DMSO solution was added. The absorbance was measured at 562 nm with a microplate reader (Thermo Scientific, Waltham, USA).

Glucose consumption

Cell suspensions of HepG2 cells in the logarithmic growth phase were prepared. The density was adjusted to 10^5 cells/mL, and 500 µL of the suspension was seeded in each well of a 24-well plate. When IR was induced in HepG2 cells by exposure to 0.3 mM PA for 24 h, the cells were transfected with SIRT1 overexpression plasmid (oe-SIRT1), Opa1 siRNA (si-Opa1), or SIRT1 siRNA (si-SIRT1) for 24 h. The cells were divided into the following groups: normal (CON); model (PA); PA + oe-SIRT1 or PA + BBR; and PA + oe-SIRT1 + si-Opa1 or PA + BBR + si-SIRT1. According to the manufacturer's instructions, the glucose content of the supernatant in triplicate wells was measured by glucose oxidase method using a glucose assay kit (NanJing JianCheng Bioengineering Institute, NanJing, China). Glucose consumption was calculated as follows: glucose consumption (mM) = glucose concentration of blank wells −

glucose concentration of wells with cells [23].

Western blot analysis

Equal amounts of proteins were separated by 10% SDS-PAGE under reducing conditions and then transferred to PVDF membranes (Merck Millipore, Darmstadt, Germany). The membranes were blocked using 5% skimmed milk in TBS supplemented with 0.1% Tween-20 and then incubated with the following antibodies: mouse anti-SIRT1 (1:1000; Abcam, Cambridge, UK), mouse anti-Drp1 (1:1000; Abcam), mouse anti-Opa1 (1:1000; Proteintech, Chicago, USA), rabbit anti-Mfn1 (1:1000; Abcam), rabbit anti-Mfn2 (1:1000; Abcam), mouse anti-NDUFA9 (1:1000; Proteintech), mouse anti-ATP5A1 (1:1000; Proteintech), rabbit anti-AKT (1:500; Santa Cruz Biotech, Santa Cruz, USA), rabbit anti-pAKT (1:500; Santa Cruz Biotech), and rabbit anti-GAPDH (1:2000; Proteintech). The signal was visualised using the corresponding horseradish peroxidase-conjugated goat anti-mouse or goat anti-rabbit secondary antibodies (1:5000; Proteintech) and enhanced chemiluminescence-western blotting detection reagent (Bioscience Biotech, Beijing, China). Protein bands were quantified by densitometry using Quantity One software.

Real-time quantitative PCR

Total RNA was extracted from liver tissues and HepG2 cells using TRIzol reagent (Invitrogen), and the isolated RNA samples were reverse transcribed using the Superscript® III first-strand synthesis system (Invitrogen). Real-time PCR was performed using the SYBR Green Mix (Roche) on the MX 3000P Real-Time PCR instrument (Agilent, Palo Alto, USA). The primer sequences are shown in **Table 1**. Data were normalised relative to those for *GAPDH* or *β-actin* expression using the $2^{-\Delta\Delta Ct}$ method.

Determination of the cellular ATP level

The ATP level was measured using a firefly luciferase-based ATP assay kit (Beyotime, Shanghai, China) according to the manufacturer's instructions. HepG2 cells were cultured and prepared as described in the "glucose consumption" section. The cells were rinsed with PBS, collected using an ATP lysing agent, and then centrifuged for 5 min at 12,000 *g* and 4°C. The supernatant was collected, and 100 µL of the supernatant was mixed with 100 µL of the ATP detection solution in a 1.5-mL tube. Luminance (RLU) was

Table 1. Sequences of primers used in this study

Gene	Primer sequence (5′→3′)
Mouse β-actin	Forward: GCTGAGAGGGAAATCGTGCGT
	Reverse: ACCGCTCGTTGCCAATAGTGA
Mouse PEPCK	Forward: AAAGCAAGACAGTCATCATCACCCA
	Reverse: TCTCAAAGTCCTCTTCCGACATCC
Mouse G6Pase	Forward: TTGCCAGGAAGAGAAAGAAGGAT
	Reverse: AACACAGACACAACTGAAGCCG
Homo GAPDH	Forward: CCATGGAGAAGGCTGGG
	Reverse: CAAAGTTGTCATGGATGACC
Homo PEPCK	Forward: AGCCTCGACAGCCTGCCCACGG
	Reverse: CCAGTTGACCAAAGGCTTTT
Homo G6Pase	Forward: ACATCCGGGGCATCTACAATG
	Reverse: AAAGAGATGCAGGCCCAA

immediately measured using an H1 synergy microplate reader (BioTek, Winooski, USA). Standard curves for the quantification were generated using an ATP standard, and the protein concentration of each treatment group was determined using the BCA protein assay kit (Thermo Scientific). Total ATP levels are expressed as NRLU (nmol/mg protein).

Assessment of mitochondrial membrane potential

The mitochondrial membrane potential assay kit (JC-1, C2006; Beyotime) was used to measure the mitochondrial membrane potential (MMP) of the HepG2 cells according to the manufacturer's instructions. Briefly, the cells were washed twice with PBS and then incubated with JC-1 at 37°C for 30 min. After incubation, the cells were washed again. An IX71 fluorescence microscope (Olympus) was used to observe the difference between green and red fluorescence. Red and green fluorescence represent high and low MMP, respectively.

Statistical analysis

Statistical analyses were performed using GraphPad Prism 5 software. Differences between the two groups were analysed using Student's t test (two-tailed). Differences between multiple groups were analysed using one-way analysis of variance, followed by Dunnett's *post hoc* test. Data are expressed as the mean ± SEM or the mean ± SD. $P < 0.05$ was considered statistically significant.

Results

Downregulation of SIRT1 and Opa1 expression was related to the imbalance of mitochondrial dynamics and hepatic IR

In this study, we used only male mice because female mice have less susceptibility to developing diabetes due to the presence of 17-β estradiol which protects pancreatic β cells from oxidative injury. The relationship between SIRT1/Opa1 signalling and hepatic IR was examined using HFD-induced obese mice. The weight and FBG of the HFD-fed mice were found to increase significantly 10 weeks after feeding on LFD and HFD (Figure 1A,B). Moreover, the HFD-fed mice exhibited impaired glucose tolerance and hyperinsulinemia (Figure 1C,D). Increased expression levels of the gluconeogenic enzymes phosphoenolpyruvate carboxykinase (PEPCK) and glucose 6-phosphatase (G6Pase) were observed (Figure 1E). The results of HE staining of the liver revealed that the cells in the HFD-fed mice were highly swollen; the cellular matrix was highly porous and showed vacuole-like changes; hepatocytes had fatty vacuoles of various sizes and clear boundaries; and hepatocyte cords were disorderly arranged, which mainly manifested as cell oedema and hepatic steatosis (Figure 1F). These results suggested that the mice had developed hepatic IR 10 weeks after feeding on an HFD.

In the HFD-fed mice, the expressions of the mitochondrial fusion proteins L-Opa1, S-Opa1, and Mfn1 were decreased, whereas that of the fission protein Drp1 was increased (Figure 2A,C–E), suggesting an imbalance in mitochondrial dynamics. The expression of SIRT1 was decreased in the HFD-fed mice (Figure 2A,B). Thus, we speculate that the downregulation of SIRT1 and Opa1 expression is related to the imbalance of mitochondrial dynamics and hepatic IR.

Opa1 deficiency changed mitochondrial fusion/fission and impaired insulin signaling in HepG2 cells

To investigate the role of Opa1 in hepatic IR, we transfected HepG2 cells with Opa1-siRNA, and the transfection efficiency was approximately 55% (Figure 3A). First, we analysed whether Opa1 deficiency causes mitochondrial dysfunction. The results showed that the expression level of the OMM fusion proteins Mfn1 and Mfn2 remained unchanged, whereas that of the fission protein Drp1 was increased (Figure 3A). The expression level of NDUFA9 (mitochondrial complex I) was decreased, whereas that of ATP5A (mitochondrial complex V) remained unchanged (Figure 3A). The ATP
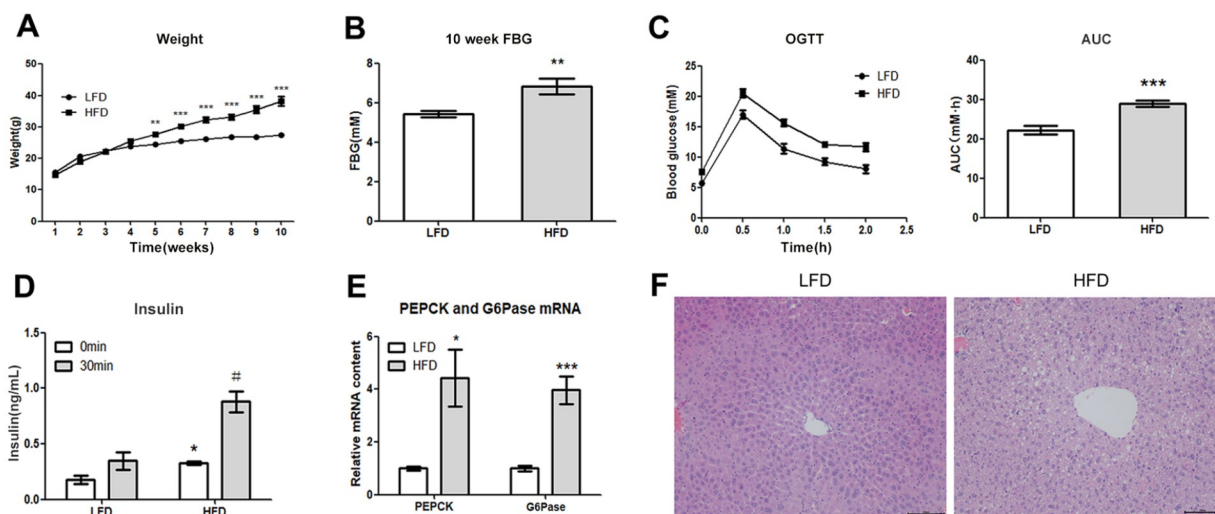
Figure 1. Establishment of an HFD-induced hepatic IR mouse model Starting from week 5, the weight of the HFD-fed mice was increased significantly. Data are expressed as the mean ± SEM (n = 10). **$P < 0.01$, ***$P < 0.001$ compared with the LFD group. (B) For HFD-fed obese mice, a significant increase in fasting blood glucose was observed at week 10. Data are expressed as the mean ± SEM (n = 6). **$P < 0.01$ compared with the LFD group. (C,D) HFD-fed mice showed impaired glucose tolerance and hyperinsulinemia. Data are expressed as the mean ± SEM (n = 6). *$P < 0.05$ compared with the LFD 0 min group; #$P < 0.05$ compared with the LFD 30 min group. (E) qPCR results showing a sharp increase in PEPCK and G6Pase expressions in the HFD-fed mice. Data are expressed as the mean ± SEM (n = 6). *$P < 0.05$, ***$P < 0.001$ compared with the LFD group. (F) HE staining results of the LFD- and HFD-fed mice liver (scale bar = 100 μm).
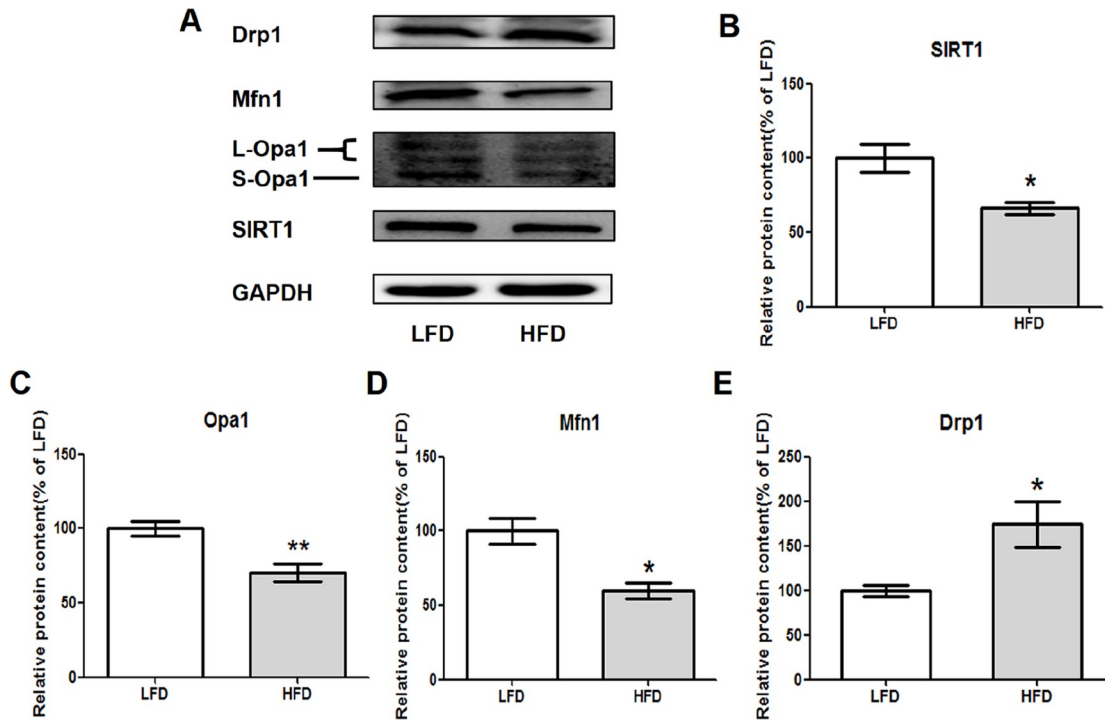
Figure 2. Downregulation of SIRT1 and Opa1 expression was related to the imbalance of mitochondrial dynamics and hepatic IR   Grayscale images of western blots of SIRT1, Opa1, Mfn1, and Drp1. (B–D) The expression levels of SIRT1, Opa1, and Mfn1 in the HFD-fed mice were decreased. Data are expressed as the mean ± SEM ($n = 3$). *$P < 0.05$, **$P < 0.01$ compared with the LFD group. (E) The expression of Drp1 in the HFD-fed mice was increased. Data are expressed as the mean ± SEM ($n = 3$). *$P < 0.05$ compared with the LFD group.
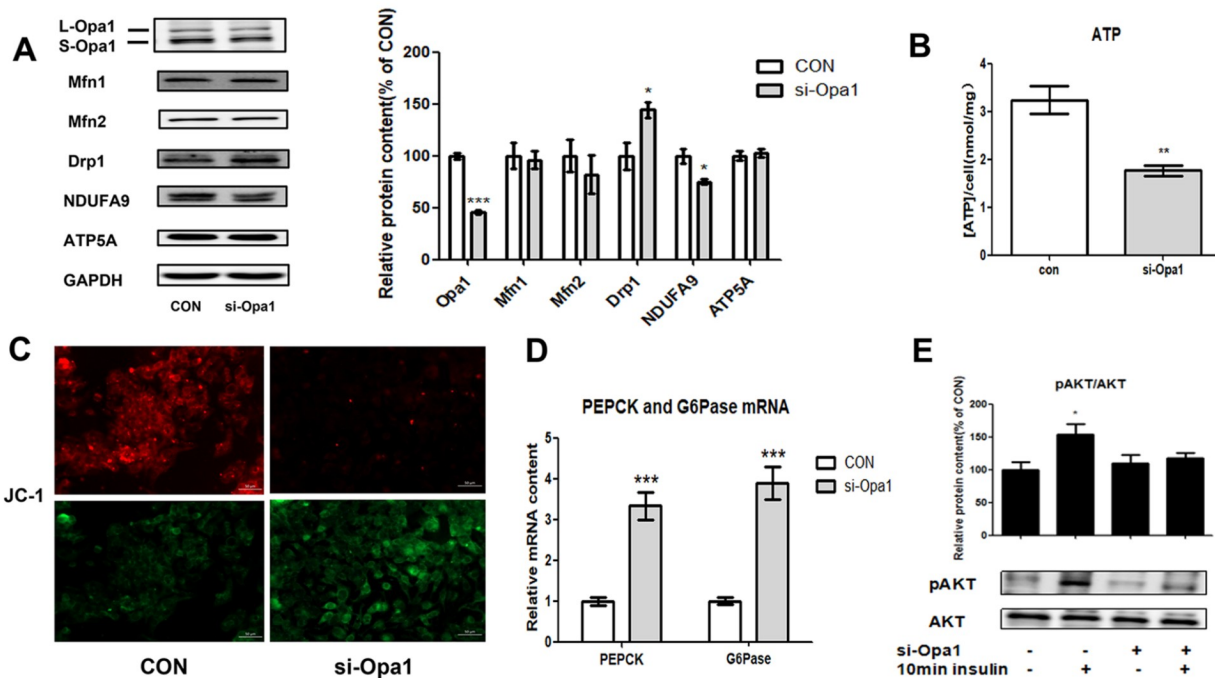
Figure 3. Opa1 deficiency changed mitochondrial fusion/fission and impaired insulin signalling in HepG2 cells   Cells were transfected with Opa1-siRNA for 48 h, and the transfection efficiency was approximately 55%. The protein expression of NDUFA9 was decreased and that of Drp1 was increased in the si-Opa1 group. (B,C) ATP content and mitochondrial membrane potential (scale bar = 50 μm) were decreased in the si-Opa1 group. Mitochondrial membrane potential in the HepG2 cells was measured by JC-1 fluorescent staining; the ratio of green fluorescence to red fluorescence represents the loss of mitochondrial membrane potential. (D) An increase in the mRNA expression of PEPCK and G6Pase was observed in the si-Opa1 group. (E) A marked reduction in AKT phosphorylation in response to insulin was observed in the si-Opa1 group. Data are expressed as the mean ± SD of 3 independent experiments with 3 determinations for each experiment. *$P < 0.05$, **$P < 0.01$, ***$P < 0.001$ compared with the si-Opa1 group.

concentration and MMP declined (Figure 3B,C) under Opal deficiency.

After transfection with Opa1-siRNA for 48 h, the two groups of cells were incubated with or without insulin (100 nM) for 10 min. IRS-2/PI3K/AKT is an important insulin signaling pathway in the liver [24], whereas AKT phosphorylation is a marker for insulin sensitivity. It was found that the control cells displayed a marked increase in AKT phosphorylation in response to insulin, and this effect was reduced in the Opa1-silenced cells (Figure 3E). Moreover, the expressions of PEPCK and G6Pase in the Opa1-silenced HepG2 cells were increased (Figure 3D).

These results suggested that Opa1 deficiency increases mitochondrial fission, decreases mitochondrial ATP concentration and membrane potential, and impairs insulin signalling and gluconeogenesis in HepG2 cells.

SIRT1 reversed hepatocyte IR and improved mitochondrial function in HepG2 cells through Opa1-mediated mitochondrial fusion

Since SIRT1 plays a key role in IR and mitochondrial biosynthesis, we analysed the relationship between SIRT1 and Opa1. First, we screened the concentration of PA and established a dose of 0.3 mM for the IR model (Figure 4A,B). Based on the IR model, we transfected the SIRT1 overexpression plasmid and Opa1-siRNA, and

observed that SIRT1 activated Opa1 in the IR model (Figure 4C,D). SIRT1 activated pAKT/AKT expression, and this activation state could be reversed after transfection with Opa1-siRNA (Figure 4E). SIRT1 overexpression also increased glucose consumption in the IR model, and this state was also reversed after transfection with Opa1-siRNA (Figure 4F). These results suggested that SIRT1 improves insulin signalling, hepatic glucose uptake, and gluconeogenesis in PA-induced IR, and these effects are achieved at least in part by Opa1 activation.

We further investigated whether SIRT1 is linked to mitochondrial function during IR. SIRT1 overexpression increased the ATP concentration and MMP (Figures 4G and 5B), whereas Opa1 silencing partly blocked these effects. Then, we investigated whether SIRT1 overexpression inhibits PA-induced mitochondrial fragmentation in HepG2 cells by visualising mitochondrial morphology with Mito-DsRed protein. As shown in Figure 5A, mitochondria of the control cells mainly appeared as elongated tubules, with highly interconnected networks. After stimulation with PA for 24 h, the volume of mitochondria was decreased, and the number of mitochondria was increased, indicating mitochondrial fragmentation. SIRT1 overexpression attenuated PA-induced mitochondrial fragmentation, which was increased after si-Opa1 transfection (Figure 5A).
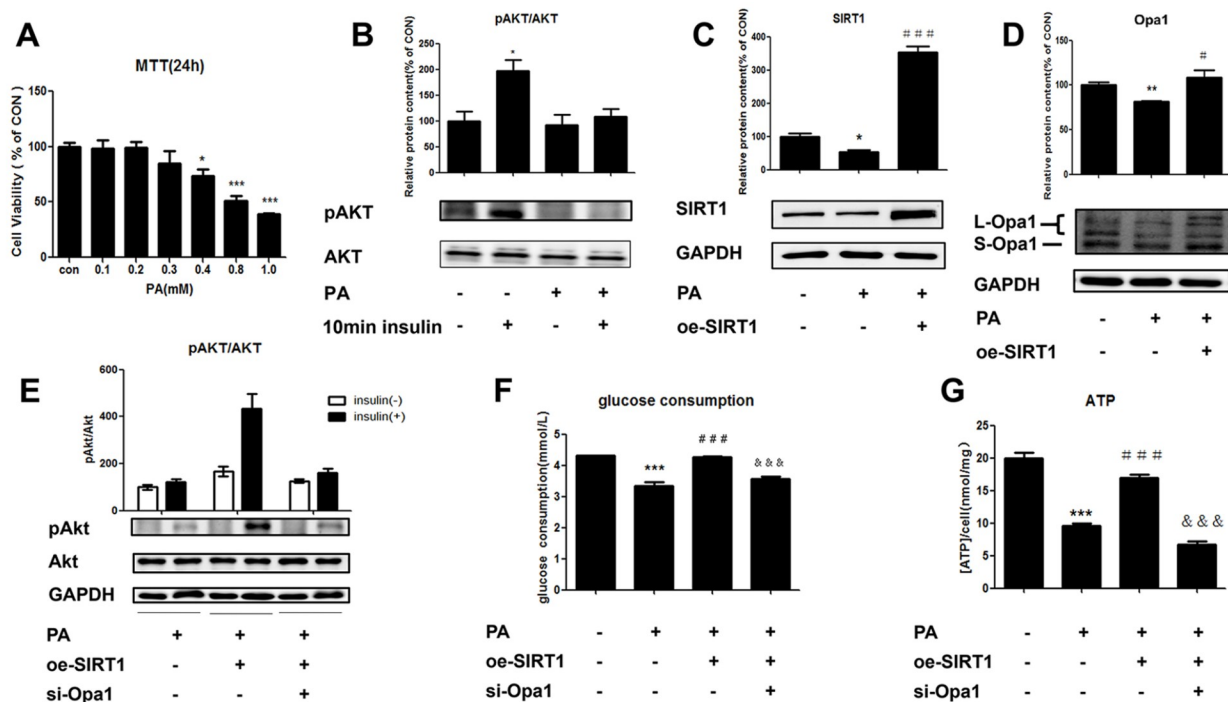
Figure 4. SIRT1 overexpression activated Opa1 and ameliorated PA-induced IR in HepG2 cells (A) The influence of PA-induced hepatic IR was assessed by the MTT assay. Data are expressed as the mean ± SD of 3 independent experiments, with 6 determinations for each experiment. *$P < 0.05$, ***$P < 0.001$ compared with the control group. (B) After treatment of HepG2 cells with 0.3 mM PA, AKT phosphorylation in response to insulin was markedly decreased, which indicated that the IR model was successfully established. Data are expressed as the mean ± SD of 3 independent experiments, with 3 determinations for each experiment. *$P < 0.05$ compared with the control group. (C,D) Protein was extracted from the cells, and the expression levels of SIRT1 and Opa1 were measured by western blot analysis. Data are expressed as the mean ± SD of 3 independent experiments, with 3 determinations for each experiment. *$P < 0.05$, **$P < 0.01$ compared with the control group; #$P < 0.05$, ###$P < 0.001$ compared with the PA group. (E) Results of AKT phosphorylation in response to insulin in each group. Data are expressed as the mean ± SD of 3 independent experiments, with 3 determinations for each experiment. (F) The glucose consumption results in each group. Data are expressed as the mean ± SD of 3 independent experiments, with 4 determinations for each experiment; ***$P < 0.001$ compared with the control group; ###$P < 0.001$ compared with the PA group; &&&$P < 0.001$ compared with the PA + oe-SIRT1 group. (G) ATP content in each group. Data are expressed as the mean ± SD of 3 independent experiments, with 3 determinations for each experiment; ***$P < 0.001$ compared with the control group; ###$P < 0.001$ compared with the PA group; &&&$P < 0.001$ compared with the PA + oe-SIRT1 group.
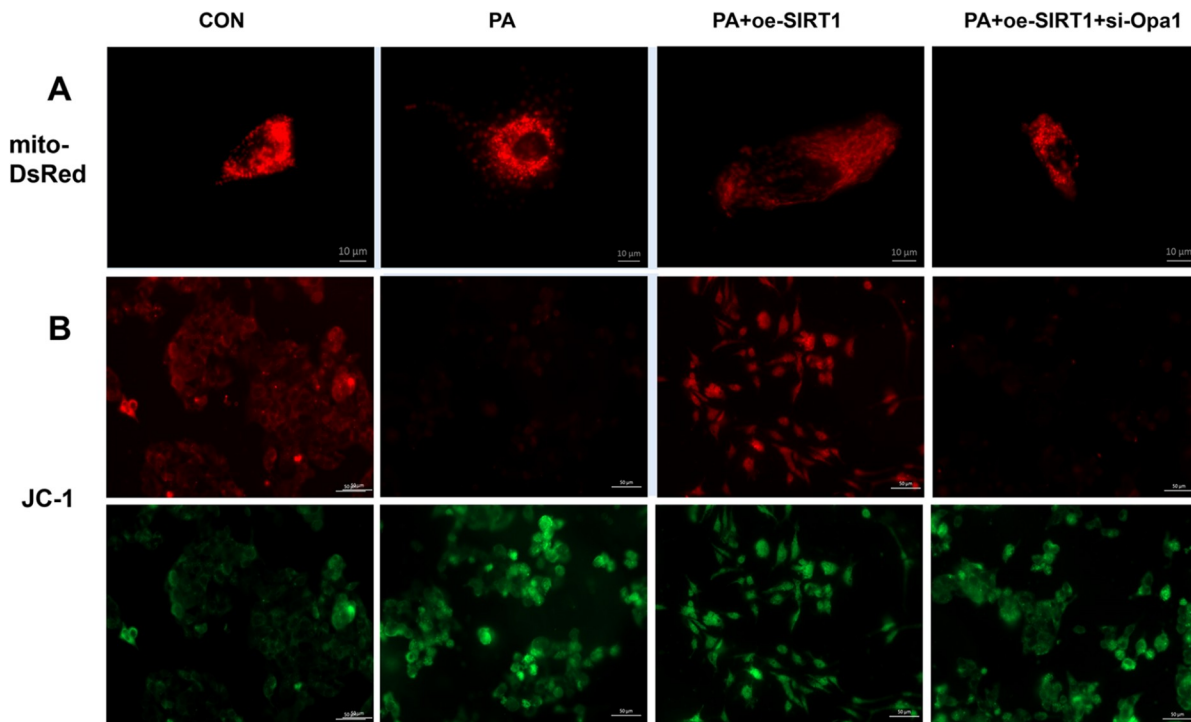
Figure 5. Overexpression of SIRT1 improved PA-induced mitochondrial morphology and mitochondrial membrane potential in HepG2 cells Mitochondrial morphology in each group transfected with mitochondrially targeted Mito-DsRed fluorescent protein (scale bar = 10 μm). (B) Mitochondrial membrane potential detected by JC-1 fluorescent staining in each group (scale bar = 50 μm).

BBR improved hepatic IR through the SIRT1/Opa1 pathway

To explore whether BBR can improve hepatic IR by regulating the SIRT1/Opa1 pathway, 10 μM BBR was administered for 24 h (Figure 6A) based on the PA model, followed by SIRT1 silencing intervention. The results revealed that when BBR was administered based on PA stimulation, SIRT1 and Opa1 protein expressions (Figure 6B,C), ATP content (Figure 6F), and MMP (Figure 6G) were all increased. Meanwhile pAKT sensitivity to insulin (Figure 6D) and glucose consumption (Figure 6E) were increased significantly. However, all these effects were attenuated after SIRT1 silencing. These results suggested that BBR improves hepatic IR by regulating the SIRT1/Opa1 pathway.

BBR improved hepatic IR and increased SIRT1 and Opa1 expressions in the livers of db/db mice

Our data revealed that the body weight, FBG, LDL, T-CHO, and TG in the db/db mice were significantly increased compared with those in the control group (Figure 7A–E). Moreover, the db/db mice exhibited impaired glucose and insulin tolerance (Figure 7F,G). Increased expression of PEPCK and G6Pase was also observed (Figure 7H,I). However, compared with the db/db group, the 4-week-old BBR-treated db/db mice exhibited significant hypoglycemic and lipid-lowering effects and an improvement in the OGTT and ITT results.

HE staining of the liver revealed that the cells in the db/db mouse liver were highly swollen, and the cellular matrix was highly porous and showed vacuole-like changes. Hepatocytes had fatty vacuoles of various sizes and clear boundaries, and the hepatocyte cords exhibited a disordered arrangement, which mainly manifested as

cell oedema and hepatic steatosis. After treament with BBR, the liver cells appeared neatly arranged and uniformly sized, the degree of lipid accumulation was significantly improved, and the degree of liver tissue damage was greatly improved (Figure 8A). As indicated by the arrows in Figure 8B, liver cell electron microscopy showed that the mitochondrial ridges in the control mouse liver cells were dense and varied in size. The volume of mitochondria in the db/db group became significantly smaller, and the ridges became sparse. Some mitochondria were broken and fused, and the condition of sparse mitochondrial cristae was significantly improved after BBR treatment.

The expression of Opa1 was decreased, whereas that of Drp1 was increased in the db/db mice, suggesting disordered mitochondrial dynamics. Additionally, the expression of SIRT1 was decreased in the db/db mice. After treatment with BBR, the expressions of SIRT1 and Opa1 were increased, whereas that of Drp1 was decreased (Figure 8C). These results suggested that the SIRT1/Opa1 pathway is related to hepatic IR.

Discussion

Excess serum free fatty acids (FFAs) play a key role in obesity and type 2 diabetes [25]. The presence of excessive FFAs in blood causes increased accumulation of lipid metabolites in the liver and skeletal muscles and can further worsen IR, which is the core defect in type 2 diabetes mellitus. Palmitate (PA), a representative saturated fatty acid, is used for the simulation of the diabetic state [26]. HepG2 cells are human-derived hepatic embryonic tumour cells with a phenotype similar to that of hepatocytes. In addition, HepG2 cells are not affected by other factors, such as ageing, and thus are used for the study of hepatic IR. In this study, we demonstrated that the
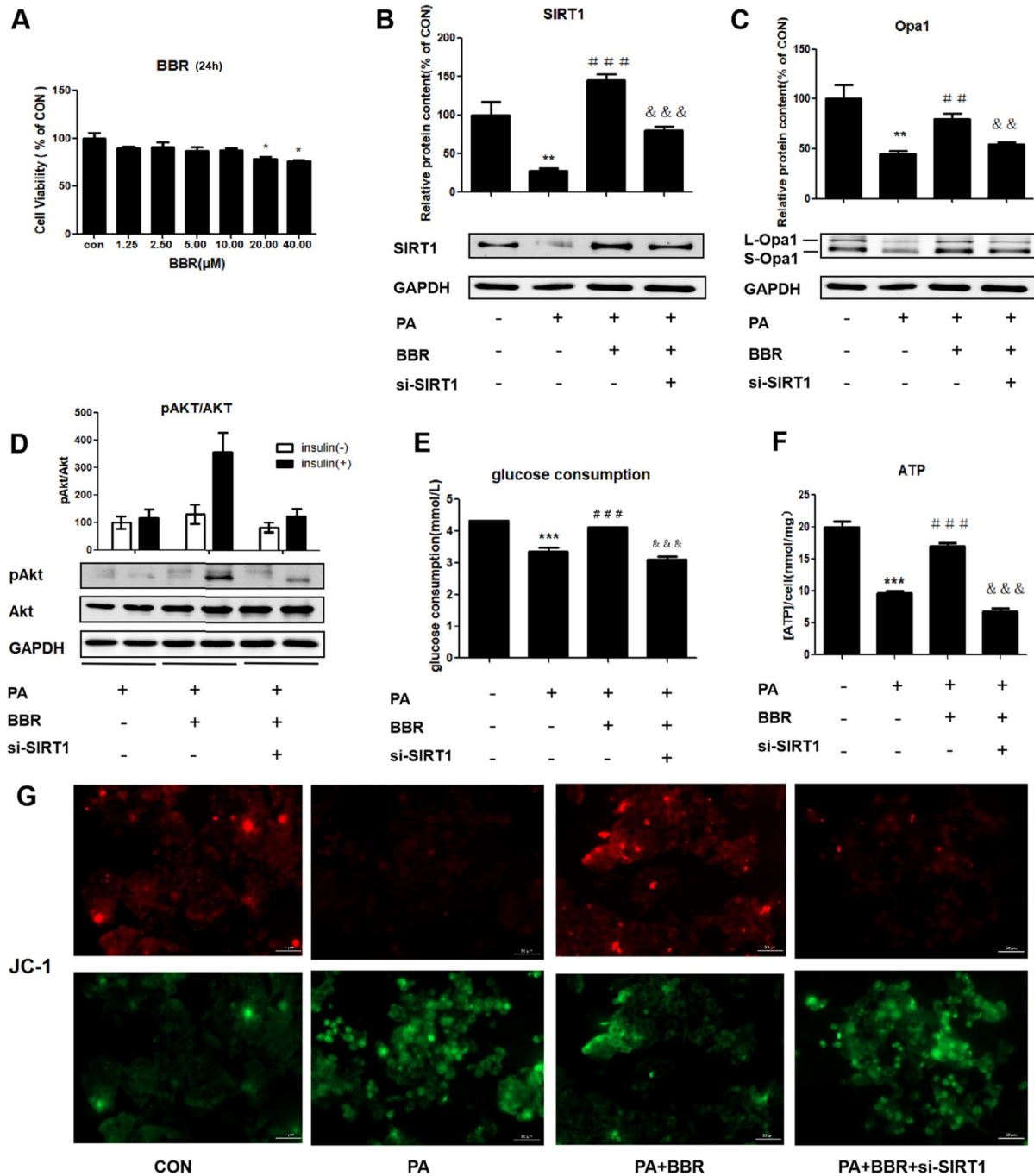
Figure 6. BBR improved hepatic IR through the SIRT1/Opa1 signalling pathway The influence of BBR on HepG2 cells was assessed by MTT assay. Data are expressed as the mean ± SD of 3 independent experiments, with 6 determinations for each experiment. *$P < 0.05$ compared with the control group. (B,C) Protein was extracted from the cells, and SIRT1 and Opa1 expressions were measured by western blot analysis. Data are expressed as the mean ± SD of 3 independent experiments, with 3 determinations for each experiment. **$P < 0.01$ compared with the control group; ##$P < 0.01$, ###$P < 0.001$ compared with the PA group; &&$P < 0.01$, &&&$P < 0.001$ compared with the PA + BBR group. (D) Results of AKT phosphorylation in response to insulin in each group. Data are expressed as the mean ± SD of 3 independent experiments, with 3 determinations for each experiment. (E) The glucose consumption results in each group. Data are expressed as the mean ± SD of 3 independent experiments, with 4 determinations for each experiment; ***$P < 0.001$ compared with the control group; ###$P < 0.001$ compared with the PA group; &&&$P < 0.001$ compared with the PA + BBR group. (F) ATP content in each group. Data are expressed as the mean ± SD of 3 independent experiments, with 3 determinations for each experiment. ***$P < 0.001$ compared with the control group; ###$P < 0.001$ compared with the PA group; &&&$P < 0.001$ compared with the PA + BBR group. (G) Mitochondrial membrane potential detected by JC-1 fluorescent staining in each group (scale bar = 50 μm).

protein expression of SIRT1/Opa1 decreases in the livers of HFD-fed mice and db/db mice and in PA-induced HepG2 cells. Opa1

silencing in HepG2 cells induced hepatocyte IR and mitochondrial dysfunction. SIRT1 overexpression and BBR treatment activated
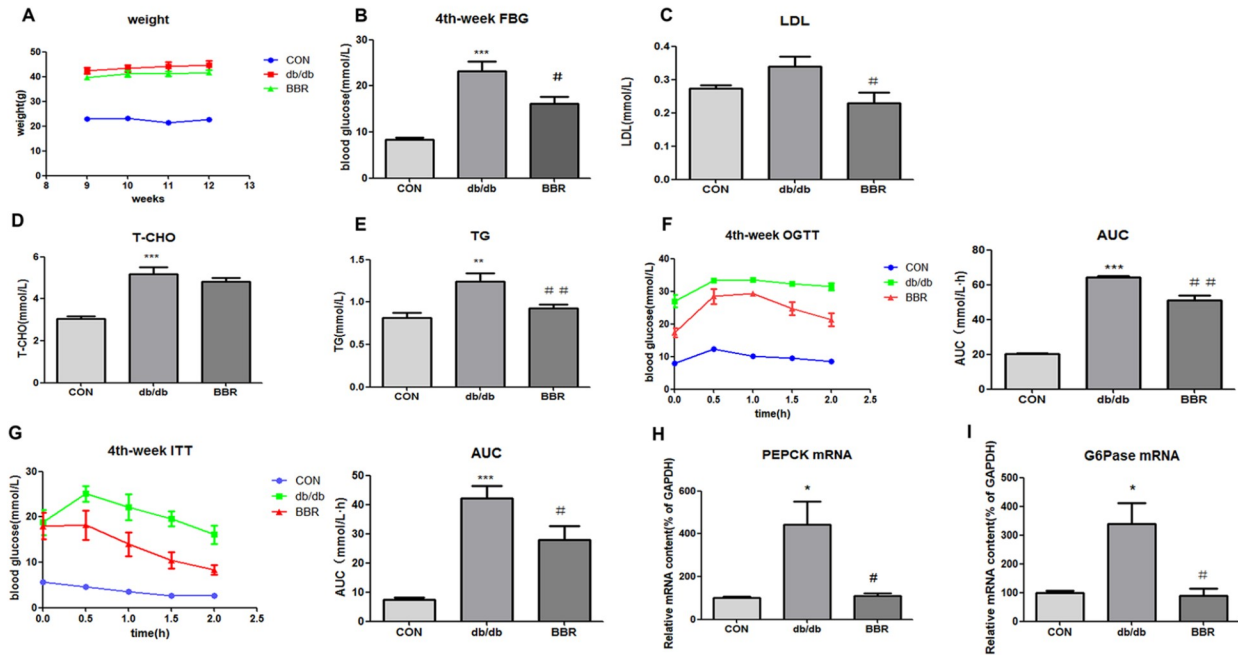
Figure 7. BBR improved hepatic IR in the db/db diabetic mice (A) Body weights were monitored for 4 weeks. (B–E) FBG, LDL, T-CHO, and TG levels were measured at the end of week 12. (F, G) Plasma glucose concentrations in different phases were measured in the oral glucose tolerance test (OGTT) and insulin tolerance test (ITT) at week 12. (H, I) qPCR results showing the mRNA expressions of PEPCK and G6Pase. Data are expressed as the mean ± SEM ($n = 6$). *$P < 0.05$, **$P < 0.01$, ***$P < 0.001$ compared with the CON group; #$P < 0.05$, ##$P < 0.01$ compared with the db/db group.
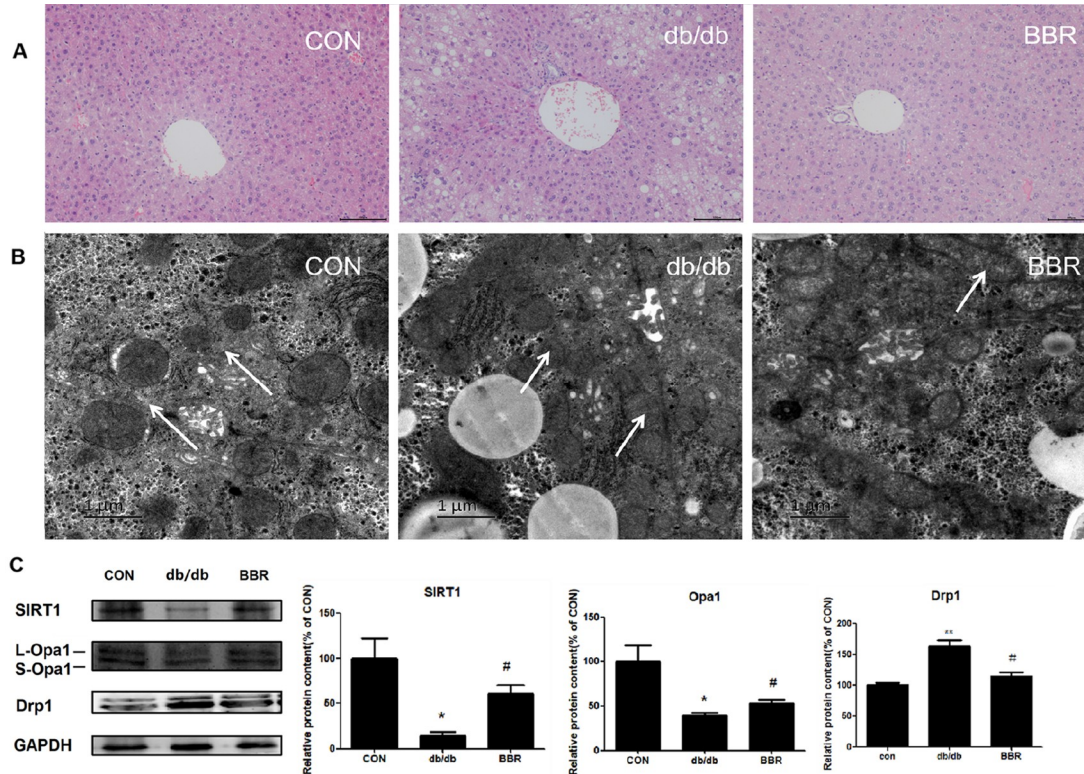
Figure 8. BBR increased SIRT1 and Opa1 expression in the livers of the db/db mice (A) HE staining of the mice liver (scale bar = 100 μm). (B) Electron microscopic images showing mitochondrial injury, which is marked with arrows (scale bar = 1 μm). (C) The expressions of SIRT1, Opa1, and Drp1 in the livers of the mice. Data are expressed as the mean ± SEM ($n = 3$). *$P < 0.05$, **$P < 0.01$ compared with the CON group; #$P < 0.05$ compared with the db/db group.

Opa1 and improved hepatocyte IR and mitochondrial functions. Opa1 and SIRT1 silencing partly reversed these effects of SIRT1 and BBR, respectively. Overall, BBR improves hepatic IR through the SIRT1/Opa1 pathway in hepatic insulin-resistant mice and PA-induced HepG2 cells. Based on these data, we propose that Opa1 is a potential target in diabetes drug development.

IR is a condition characterised by the decreased sensitivity of peripheral tissues (liver, muscle, and adipose tissues) to insulin [27]. Given the key role of the liver in glucose production and lipid metabolism, hepatic IR is considered to be involved in the development of IR and diabetes [28]. Therefore, a better under-standing of the mechanism of hepatic IR may help in elucidating a new therapeutic target for the treatment and prevention of diabetes. Insulin binds to the insulin receptor and promotes the autopho-sphorylation of IR tyrosine residues in hepatocytes [29,30]. Then, tyrosine kinase phosphorylates insulin receptor substrate 2 (IRS-2), which can further activate phosphatidylinositol 3-kinase (PI3K) and AKT/protein kinase B and promote glucose transporter 2 (GLUT2) membrane transport. The insulin signaling pathway promotes blood glucose entry into hepatocytes and regulates the normal metabolism of lipids and glucose [31,32]. Excessive lipid accumula-tion in the liver may impair the hepatic insulin signalling pathway and cause hepatic IR [33]. In our study, the HFD-fed mice and db/db mice exhibited increased FBG, impaired glucose tolerance, hyper-insulinemia, and high expression of gluconeogenic enzymes (PEPCK and G6Pase). Additionally, PA-treated HepG2 cells demon-strated AKT insensitivity in response to insulin and decreased glucose consumption, indicating that the IR cell model can be successfully constructed using HepG2 cells. Mitochondrial dy-namics imbalance is the main cause of peripheral IR and type 2 diabetes [34–36]. Our results also validate the abnormality of mitochondrial fusion and fission during hepatic IR. BBR and SIRT1 play an important role in the preservation of mitochondrial dynamics and improvement of hepatic IR.

Opa1 is a GTPase anchored to the IMM that exists in long and short isoforms. In addition to being responsible for the IMM fusion, Opa1 is involved in maintaining the crista structure and protecting cells from apoptosis [37,38]. Opa1 deficiency is closely related to the occurrence and development of diabetes. Zhang et al. [39] reported that Opa1 deficiency in pancreatic β cells impaired glucose-stimulated ATP production and insulin secretion, which eventually resulted in the development of hyperglycaemia. Ding et al. [40] reported that Opa1 expression was reduced in the hearts of diabetic rats, and after treatment with the mitochondrial fusion activator M1, Opa1 expression was increased, and mitochondrial function and diabetic cardiomyopathy were improved; however, all these effects were weakened after Opa1 silencing. As shown in Figure 3A, the effect of siRNA Opa1 was limited to S-Opa1, but the down-regulation of L-Opa1 and S-Opa1 expression was observed in the HFD-fed mice (Figure 2A) and PA-treated HepG2 cells (Figure 4D). Furthermore, we observed increased expressions of gluconeogenic genes, such as PEPCK and G6Pase, in Opa1-silenced HepG2 cells. The sensitivity of AKT to insulin was also reduced in Opa1-silenced HepG2 cells. Therefore, we infer that Opa1 deficiency is associated with a pattern of hepatic IR in animal and cell models. Under these conditions, we also observed that Opa1 deficiency affects mito-chondrial fusion and fission processes. Further studies are required to explore whether Opa1 deficiency reduces insulin signalling in liver tissues and induces susceptibility to IR in Opa1 liver-KO mice

and to specifically probe the role played by L-Opa1 and S-Opa1.

The human sirtuin isoforms SIRT1-7 have been found to be related to type-2 diabetes [41]. SIRT2 is mainly distributed in the cytoplasm; SIRT1, SIRT6, and SIRT7 are mainly distributed in the nucleus, and SIRT3, SIRT4, and SIRT5 are distributed in the mitochondria. Previous studies have shown that SIRT3 regulates mitochondrial dynamics by deacetylating and activating Opa1 during stress [42], whereas SIRT4 regulates mitochondrial quality control and mitophagy by interacting with Opa1 [43]. SIRT5 overexpression prevents mitochondrial fragmentation and protects against mitophagy by increasing Mfn2 and Opa1 expression, whereas these effects are reversed after SIRT5 silencing [44]. However, evidence to confirm that SIRT1 regulates Opa1 is lacking. Another major finding of our study is that SIRT1 activates Opa1, improves hepatic IR, inhibits PA-induced mitochondrial fragmenta-tion, and alleviates mitochondrial dysfunction in PA-induced HepG2 cells. These effects are partly reversed when Opa1 is silenced. Thus, the activation of Opa1 by SIRT1 plays a key role in alleviating hepatocyte IR.

BBR has received increasing attention for its potential to treat liver steatosis, dyslipidaemia, and diabetes. BBR and its derivatives have been shown to reduce hepatic steatosis in HepG2 cells [45], HFD-fed rats [46–48], and patients with nonalcoholic fatty liver [49], and SIRT1 is the key regulator in liver lipid metabolism [50]. Therefore, to investigate whether BBR can reduce blood glucose and improve hepatic IR through SIRT1 and whether SIRT1 is related to mitochondrial dynamics-related proteins, we performed SIRT1 silencing to observe the relationship of SIRT1 with Opa1 in PA-induced HepG2 cells. The results revealed that BBR increased SIRT1 and Opa1 protein expressions, ATP content, and MMP. The sensitivity of pAKT to insulin and glucose consumption were significantly increased. However, these effects were reversed after SIRT1 silencing, suggesting that BBR improves hepatic IR by upregulating the SIRT1/Opa1 pathway.

To validate the effect in vivo, we treated db/db mice with BBR. The results revealed that BBR treatment significantly improved the blood glucose level and liver IR of the mice. The expressions of Opa1 and SIRT1 were upregulated after BBR treatment, whereas the expression of Drp1 was downregulated. Mitochondrial frag-mentation was significantly decreased after BBR treatment. BBR improves the development of hepatic IR, which may be related to the balance of mitochondrial dynamics and upregulation of the SIRT1/Opa1 signalling pathway (Figure 9). Overall, these results
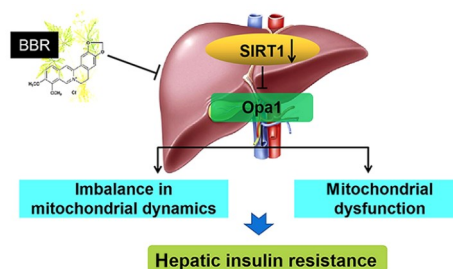
Figure 9. BBR mitigates hepatic insulin resistance by enhancing mitochondrial architecture via the SIRT1/Opa1 signalling pathway Opa1 deficiency in the liver triggers mitochondrial fusion/fission imbalance and mitochondrial dysfunction, which leads to hepatic IR. BBR may improve hepatic IR by regulating the SIRT1/Opa1 signaling pathway.

suggest that BBR can improve hepatic IR by regulating the SIRT1/Opa1 pathway in db/db mice and PA-treated HepG2 cells. It has been suggested that BBR could stimulate mitochondrial biogenesis via SIRT1 or attenuate hepatic IR through the miR-146b/SIRT1 pathway [21,51]. Therefore, we speculate that BBR improves hepatic IR via the miR-146b/SIRT1/Opa1 signalling pathway directly or indirectly. A limitation of our study is that the effect of BBR on SIRT1-dependent gene expression was not analysed. In our future studies, we will confirm the mechanism through which SIRT1 regulates Opa1.

In summary, our results showed that Opa1 silencing-mediated mitochondrial fusion/fission imbalance could lead to hepatocyte IR, whereas SIRT1 improves hepatocyte IR by activating Opa1. As an effective hypoglycemic drug, BBR may improve hepatic IR by regulating the SIRT1/Opa1 signaling pathway and thus can be used to treat type-2 diabetes.

Conflict of Interest
The authors declare that they have no conflict of interest.

References
1. Srinivasan S, Guha M, Kashina A, Avadhani NG. Mitochondrial dysfunction and mitochondrial dynamics—the cancer connection. *Biochim Biophys Acta Bioenerg* 2017, 1858: 602–614
2. Liesa M, Shirihai OS. Mitochondrial dynamics in the regulation of nutrient utilization and energy expenditure. *Cell Metab* 2013, 17: 491–506
3. Bianco F, Mazzoli A, Giacco A, Liverini G, Iossa S. A possible link between hepatic mitochondrial dysfunction and diet-induced insulin resistance. *Eur J Nutr* 2016, 55: 1–6
4. Rovira-Llopis S, Bañuls C, Diaz-Morales N, Hernandez-Mijares A, Rocha M, Victor VM. Mitochondrial dynamics in type 2 diabetes: pathophysiological implications. *Redox Biol* 2017, 11: 637–645
5. Kulkarni SS, Joffraud M, Boutant M, Ratajczak J, Gao AW, Maclachlan C, Hernandez-Alvarez MI, *et al.* Mfn1 deficiency in the liver protects against diet-induced insulin resistance and enhances the hypoglycemic effect of metformin. *Diabetes* 2016, 65: 3552–3560
6. Sebastián D, Hernández-Alvarez MI, Segalés J, Sorianello E, Muñoz JP, Sala D, Waget A, *et al.* Mitofusin 2 (Mfn2) links mitochondrial and endoplasmic reticulum function with insulin signaling and is essential for normal glucose homeostasis. *Proc Natl Acad Sci USA* 2012, 109: 5523–5528
7. Wang L, Ishihara T, Ibayashi Y, Tatsushima K, Setoyama D, Hanada Y, Takeichi Y, *et al.* Disruption of mitochondrial fission in the liver protects mice from diet-induced obesity and metabolic deterioration. *Diabetologia* 2015, 58: 2371–2380
8. Lee H, Yoon Y. Mitochondrial membrane dynamics—functional positioning of OPA1. *Antioxidants* 2018, 7: 186
9. Lee H, Smith SB, Sheu SS, Yoon Y. The short variant of optic atrophy 1 (OPA1) improves cell survival under oxidative stress. *J Biol Chem* 2020, 295: 6543–6560
10. Ban T, Ishihara T, Kohno H, Saita S, Ichimura A, Maenaka K, Oka T, *et al.* Molecular basis of selective mitochondrial fusion by heterotypic action between OPA1 and cardiolipin. *Nat Cell Biol* 2017, 19: 856–863
11. Griparic L, Kanazawa T, van der Bliek AM. Regulation of the mitochondrial dynamin-like protein Opa1 by proteolytic cleavage. *J Cell Biol* 2007, 178: 757–764
12. Yuan Y, Cruzat VF, Newsholme P, Cheng J, Chen Y, Lu Y. Regulation of SIRT1 in aging: roles in mitochondrial function and biogenesis. *Mech Ageing Dev* 2016, 155: 10–21
13. Sui M, Chen G, Mao X, Wei X, Chen Y, Liu C, Fan Y. Gegen qinlian decoction ameliorates hepatic insulin resistance by silent information regulator1 (SIRT1)-dependent deacetylation of forkhead Box O1 (FOXO1). *Med Sci Monit* 2019, 25: 8544–8553
14. Jung TW, Ahn SH, Shin JW, Kim HC, Park ES, Abd El-Aty AM, Hacımüftüoğlu A, *et al.* Protectin DX ameliorates palmitate-induced hepatic insulin resistance through AMPK/SIRT1-mediated modulation of fetuin-A and SeP expression. *Clin Exp Pharmacol Physiol* 2019, 46: 898–909
15. Kitada M, Koya D. SIRT1 in type 2 diabetes: mechanisms and therapeutic potential. *Diabetes Metab J* 2013, 37: 315–325
16. Ding M, Feng N, Tang D, Feng J, Li Z, Jia M, Liu Z, *et al.* Melatonin prevents Drp1-mediated mitochondrial fission in diabetic hearts through SIRT1-PGC1α pathway. *J Pineal Res* 2018, 65: e12491
17. Battu SK, Repka MA, Maddineni S, Chittiboyina AG, Avery MA, Majumdar S. Physicochemical characterization of berberine chloride: a perspective in the development of a solution dosage form for oral delivery. *AAPS PharmSciTech* 2010, 11: 1466–1475
18. Xu Z, Feng W, Shen Q, Yu N, Yu K, Wang S, Chen Z, *et al.* Rhizoma coptidis and berberine as a natural drug to combat aging and aging-related diseases via anti-oxidation and AMPK activation. *Aging Dis* 2017, 8: 760–777
19. Tu J, Zhu S L, Zhou X M. Differentiated hypoglycemic effects of baicalin, berberine and puerarin on insulin-resistance HepG2 cells. *China J Chi Mat Med* 2018, 43: 4097–4103
20. Qin X, Zhao Y, Gong J, Huang W, Su H, Yuan F, Fang K, *et al.* Berberine protects glomerular podocytes via inhibiting Drp1-mediated mitochondrial fission and dysfunction. *Theranostics* 2019, 9: 1698–1713
21. Gomes AP, Duarte FV, Nunes P, Hubbard BP, Teodoro JS, Varela AT, Jones JG, *et al.* Berberine protects against high fat diet-induced dysfunction in muscle mitochondria by inducing SIRT1-dependent mitochondrial biogenesis. *Biochim Biophys Acta* 2012, 1822: 185–195
22. Zhang M, Lv X, Li J, Meng Z, Wang Q, Chang WG, Li W, *et al.* Sodium caprate augments the hypoglycemic effect of berberine via AMPK in inhibiting hepatic gluconeogenesis. *Mol Cell Endocrinol* 2012, 363: 122–130
23. Si M, Yan Y, Tang L, Wu H, Yang B, He Q, Wu H. A novel indole derivative compound GY3 improves glucose and lipid metabolism via activation of AMP-activated protein kinase pathway. *Eur J Pharmacol* 2013, 698: 480–488
24. Petersen MC, Shulman GI. Mechanisms of insulin action and insulin resistance. *Physiol Rev* 2018, 98: 2133–2223
25. Daniele G, Eldor R, Merovci A, Clarke GD, Xiong J, Tripathy D, Taranova A, *et al.* Chronic reduction of plasma free fatty acid improves mitochondrial function and whole-body insulin sensitivity in obese and type 2 diabetic individuals. *Diabetes* 2014, 63: 2812–2820
26. Yang Z, Chen X, Chen Y, Zhao Q. Decreased irisin secretion contributes to muscle insulin resistance in high-fat diet mice. *Int J Clin Exp Pathol* 2015, 8: 6490-6497
27. Barseem NF, Helwa MA. Homeostatic model assessment of insulin

resistance as a predictor of metabolic syndrome: consequences of obesity in children and adolescents. *Egyptian Pediatr Assoc Gazette* 2015, 63: 19–24

28. Ibarra-Reynoso LR, Pisarchyk L, Pérez-Luque EL, Garay-Sevilla ME, Malacara JM. Whole-body and hepatic insulin resistance in obese children. *PLoS ONE* 2014, 9: e113576

29. Morakinyo AO, Samuel TA, Adekunbi DA. Magnesium upregulates insulin receptor and glucose transporter-4 in streptozotocin-nicotinamide-induced type-2 diabetic rats. *Endocr Regul* 2018, 52: 6–16

30. Wang J, Zou T, Yang HX, Gong YZ, Xie XJ, Liu HY, Liao DF. Insulin receptor binding motif tagged with IgG4 Fc (Yiminsu) works as an insulin sensitizer to activate AKT signaling in hepatocytes. *Genet Mol Res* 2015, 14: 8819–8828

31. Cai S, Sun W, Fan Y, Guo X, Xu G, Xu T, Hou Y, *et al.* Effect of mulberry leaf (*Folium Mori*) on insulin resistance via IRS-1/PI3K/Glut-4 signalling pathway in type 2 diabetes mellitus rats. *Pharm Biol* 2016, 54: 2685–2691

32. Chen L, Zheng S, Huang M, Ma X, Yang J, Deng S, Huang Y, *et al.* β-ecdysterone from *Cyanotis arachnoidea* exerts hypoglycemic effects through activating IRS-1/Akt/GLUT4 and IRS-1/Akt/GLUT2 signal pathways in KK-Ay mice. *J Funct Foods* 2017, 39: 123–132

33. Chen L, Chen XW, Huang X, Song BL, Wang Y, Wang Y. Regulation of glucose and lipid metabolism in health and disease. *Sci China Life Sci* 2019, 62: 1420–1458

34. Zorzano A, Liesa M, Palacín M. Mitochondrial dynamics as a bridge between mitochondrial dysfunction and insulin resistance. *Arch Physiol Biochem* 2009, 115: 1–12

35. Roy M, Reddy PH, Iijima M, Sesaki H. Mitochondrial division and fusion in metabolism. *Curr Opin Cell Biol* 2015, 33: 111–118

36. Wang CH, Wang CC, Wei YH. Mitochondrial dysfunction in insulin insensitivity: implication of mitochondrial role in type 2 diabetes. *Ann New York Acad Sci* 2010, 1201: 157–165

37. Frezza C, Cipolat S, Martins de Brito O, Micaroni M, Beznoussenko GV, Rudka T, Bartoli D, *et al.* OPA1 controls apoptotic cristae remodeling independently from mitochondrial fusion. *Cell* 2006, 126: 177–189

38. Olichon A, Baricault L, Gas N, Guillou E, Valette A, Belenguer P, Lenaers G. Loss of OPA1 perturbates the mitochondrial inner membrane structure and integrity, leading to cytochrome c release and apoptosis. *J Biol Chem* 2003, 278: 7743–7746

39. Zhang Z, Wakabayashi N, Wakabayashi J, Tamura Y, Song WJ, Sereda S, Clerc P, *et al.* The dynamin-related GTPase Opa1 is required for glucose-stimulated ATP production in pancreatic beta cells. *Mol Biol Cell* 2011, 22: 2235–2245

40. Ding M, Liu C, Shi R, Yu M, Zeng K, Kang J, Fu F, *et al.* Mitochondrial fusion promoter restores mitochondrial dynamics balance and ameliorates diabetic cardiomyopathy in an optic atrophy 1-dependent way. *Acta Physiol* 2020, 229: e13428

41. Farghali H, Kemelo MK, Canová NK. SIRT1 modulators in experimentally induced liver injury. *Oxid Med Cell Longev* 2019, 2019: 1–15

42. Samant SA, Zhang HJ, Hong Z, Pillai VB, Sundaresan NR, Wolfgeher D, Archer SL, *et al.* SIRT3 deacetylates and activates OPA1 to regulate mitochondrial dynamics during stress. *Mol Cell Biol* 2014, 34: 807–819

43. Lang A, Anand R, Altinoluk-Hambüchen S, Ezzahoini H, Stefanski A, Iram A, Bergmann L, *et al.* SIRT4 interacts with OPA1 and regulates mitochondrial quality control and mitophagy. *Aging* 2017, 9: 2163–2189

44. Polletta L, Vernucci E, Carnevale I, Arcangeli T, Rotili D, Palmerio S, Steegborn C, *et al.* SIRT5 regulation of ammonia-induced autophagy and mitophagy. *Autophagy* 2015, 11: 253–270

45. Brusq JM, Ancellin N, Grondin P, Guillard R, Martin S, Saintillan Y, Issandou M. Inhibition of lipid synthesis through activation of AMP kinase: an additional mechanism for the hypolipidemic effects of berberine. *J Lipid Res* 2006, 47: 1281–1288

46. Chang XX, Yan HM, Fei J, Jiang MH, Zhu HG, Lu DR, Gao X. Berberine reduces methylation of the MTTP promoter and alleviates fatty liver induced by a high-fat diet in rats. *J Lipid Res* 2010, 51: 2504–2515

47. Xia X, Yan J, Shen Y, Tang K, Yin J, Zhang Y, Yang D, *et al.* Berberine improves glucose metabolism in diabetic rats by inhibition of hepatic gluconeogenesis. *PLoS ONE* 2011, 6: e16556

48. Yuan X, Wang J, Tang X, Li Y, Xia P, Gao X. Berberine ameliorates nonalcoholic fatty liver disease by a global modulation of hepatic mRNA and lncRNA expression profiles. *J Transl Med* 2015, 13: 24

49. Yan HM, Xia MF, Wang Y, Chang XX, Yao XZ, Rao SX, Zeng MS, *et al.* Efficacy of berberine in patients with non-alcoholic fatty liver disease. *PLoS ONE* 2015, 10: e0134172

50. Sun Y, Xia M, Yan H, Han Y, Zhang F, Hu Z, Cui A, *et al.* Berberine attenuates hepatic steatosis and enhances energy expenditure in mice by inducing autophagy and fibroblast growth factor 21. *Br J Pharmacol* 2018, 175: 374–387

51. Sui M, Jiang X, Sun H, Liu C, Fan Y. Berberine ameliorates hepatic insulin resistance by regulating microRNA-146b/SIRT1 pathway. *Diabetes Metab Syndr Obes* 2021, 14: 2525–2537